Supplementary information for

Evidence of extremely short hydrogen bond in homoconjugated anion of ferrocene-1,1′-diyl-bisphosphinic acid: sign change of H/D isotope effect on the ^{31}P NMR chemical shift

E.R. Chakalov[a], R.P. Shekurov[b], V.A. Miluykov[b] and P.M. Tolstoy*[a]

[a] *Institute of Chemistry, St. Petersburg State University, 198504 St. Petersburg, Russia*

[b] *A.E. Arbuzov Institute of Organic and Physical Chemistry, RAS, 420088 Kazan, Russia*

* – *corresponding author*: peter.tolstoy@spbu.ru

Contents	Page

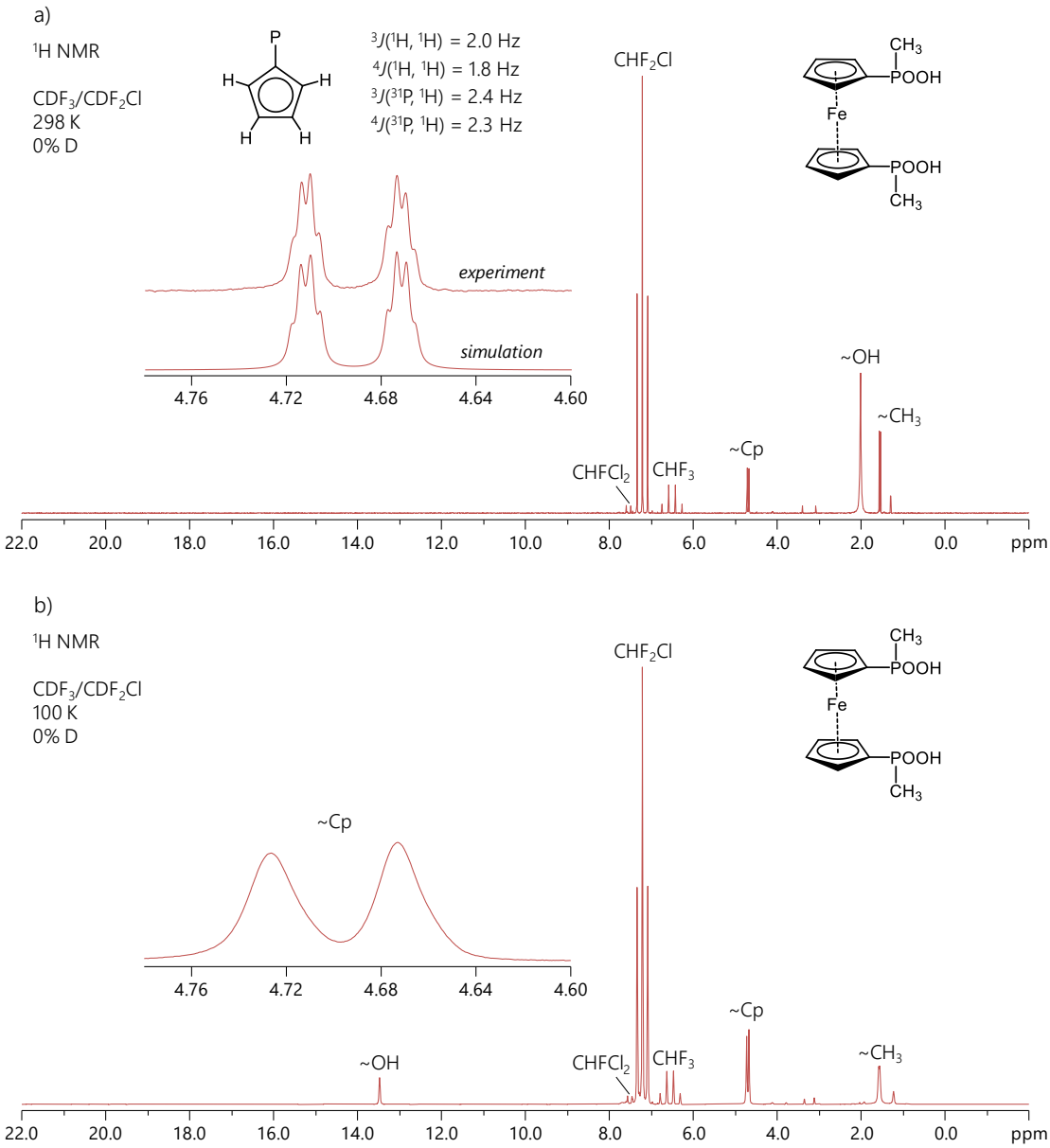

Figure S1. Overview ^{1}H NMR spectra of the non-deuterated FcPMe in a CDF_3/CDF_2Cl solution at 298 K (a) and 100 K (b). In the inset of Figure S1a are depicted the experimental and simulated multiplet structures of the FcPMe cyclopentadienyl protons' signals with corresponding *J*-coupling constants at 298 K. The vanishing of a multiplet structure at 100 K is caused by the transverse relaxation time T_2 decrease due to an increase in molecular motion correlation time τ_c with an increase in solution viscosity.

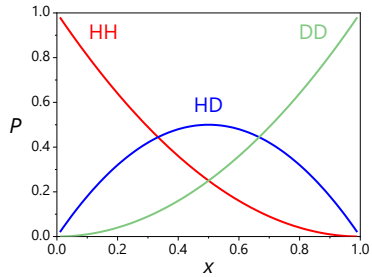

$P_{HH} = (1-x)^2$

$P_{HD} = 2\cdot(1-x)\cdot x$

$P_{DD} = x^2$

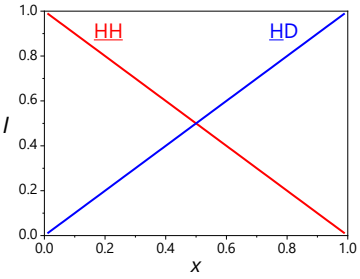

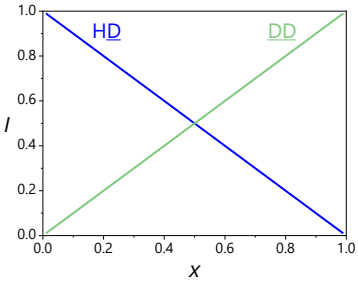

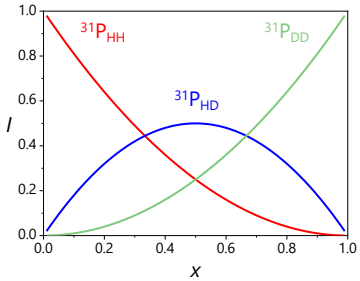

$I_{\underline{HH}} = 2\cdot P_{HH} = 2\cdot(1-x)^2$

$I_{\underline{H}D} = P_{HD} = 2\cdot(1-x)\cdot x$

$I_{H\underline{D}} = P_{HD} = 2\cdot(1-x)\cdot x$

$I_{\underline{DD}} = 2\cdot P_{DD} = 2\cdot x^2$

$I(^{31}P_{HH}) = 2\cdot P_{HH} = 2\cdot(1-x)^2$

$I(^{31}P_{HD}) = 2\cdot P_{HD} = 4\cdot(1-x)\cdot x$

$I(^{31}P_{DD}) = 2\cdot P_{DD} = 2\cdot x^2$

$$I_{\underline{HH},\,\mathrm{rel.}} = \frac{I_{\underline{HH}}}{I_{\underline{HH}} + I_{\underline{H}D}} = 1-x$$

$$I_{\underline{H}D,\,\mathrm{rel.}} = \frac{I_{\underline{H}D}}{I_{\underline{HH}} + I_{\underline{H}D}} = x$$

$$I_{H\underline{D},\,\mathrm{rel.}} = \frac{I_{H\underline{D}}}{I_{H\underline{D}} + I_{\underline{DD}}} = 1-x$$

$$I_{\underline{DD},\,\mathrm{rel.}} = \frac{I_{\underline{DD}}}{I_{H\underline{D}} + I_{\underline{DD}}} = x$$

$$I(^{31}P_{HH})_{\mathrm{rel.}} = \frac{I(^{31}P_{HH})}{I(^{31}P_{HH}) + I(^{31}P_{HD}) + I(^{31}P_{DD})} = (1-x)^2$$

$$I(^{31}P_{HD})_{\mathrm{rel.}} = \frac{I(^{31}P_{HD})}{I(^{31}P_{HH}) + I(^{31}P_{HD}) + I(^{31}P_{DD})} = 2\cdot(1-x)\cdot x$$

$$I(^{31}P_{DD})_{\mathrm{rel.}} = \frac{I(^{31}P_{DD})}{I(^{31}P_{HH}) + I(^{31}P_{HD}) + I(^{31}P_{DD})} = x^2$$

Figure S2. The probabilities *P* (top) of various isotopologues of the FcPMe intramolecular cyclic dimer and their relative integral intensities *I* (bottom) in the ^{1}H (left), ^{2}H (center) and ^{31}P (right) NMR spectra as functions of the deuteration degree *x*.

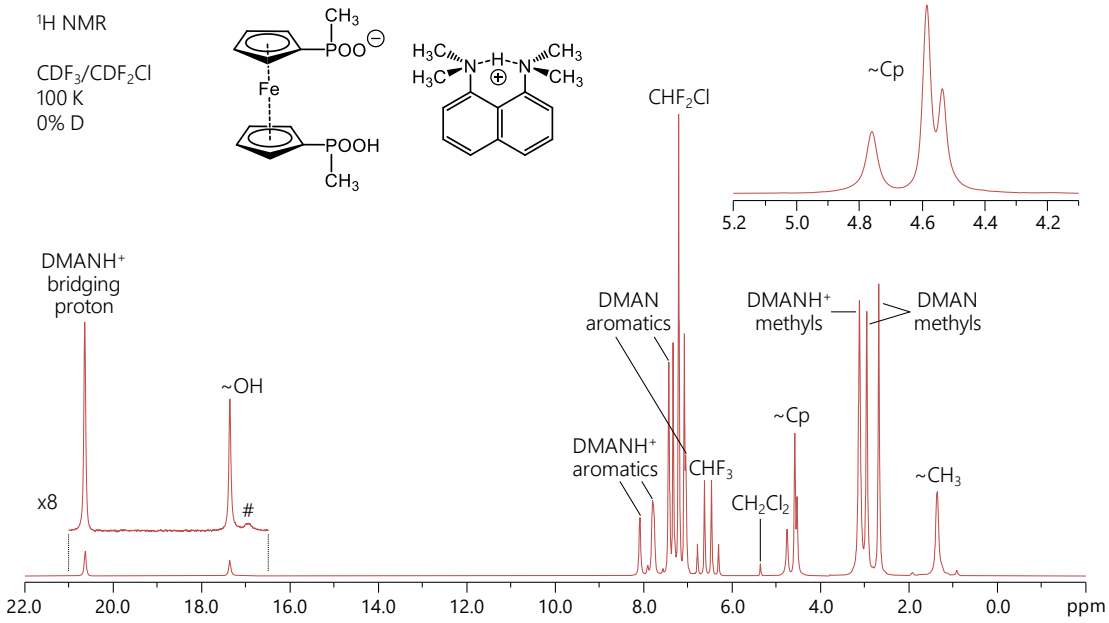

Figure S3. Overview ^{1}H NMR spectrum of the non-deuterated mixture of FcPMe with DMAN (ca. 1 :1.5 molar ratio) in a CDF_3/CDF_2Cl solution at 100 K. The ^{1}H signal marked with a hash was tentatively assigned to the double monoanion of FcPMe (please refer to the main text for clarification).

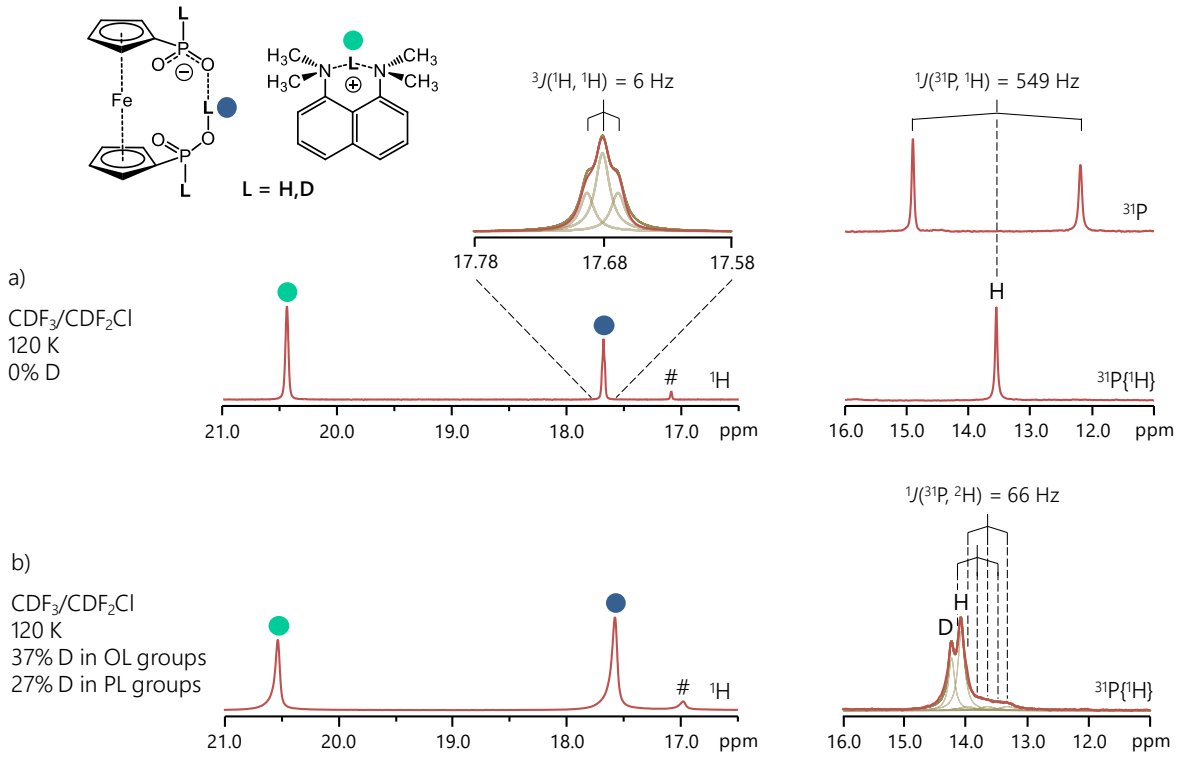

Figure S4. ^{1}H (low-field part), ^{31}P and ^{31}P{^{1}H} NMR spectra of the FcPH with DMAN mixture in a CDF_3/CDF_2Cl solution at 120 K. The spectra correspond to the non-deuterated (a) (ca. 1 : 4 molar ratio) and partially deuterated (b) (ca. 1 : 1 molar ratio) samples. The deuteration degrees of O–H and P–H groups are 37% and 27%, respectively. Similarly, the ^{1}H signal marked with a hash was tentatively assigned to the double monoanion of FcPH (please refer to the main text for clarification). An offset in signal positions of the non-deuterated molecular species is associated with the solvent composition variation. Asymmetry of the coupled ^{31}P signals of the non-deuterated sample is caused by differential line broadening (see, for example, [Farrar et al. *eMagRes*, John Wiley & Sons, Ltd, 2007. DOI: 10.1002/9780470034590.emrstm0465]).

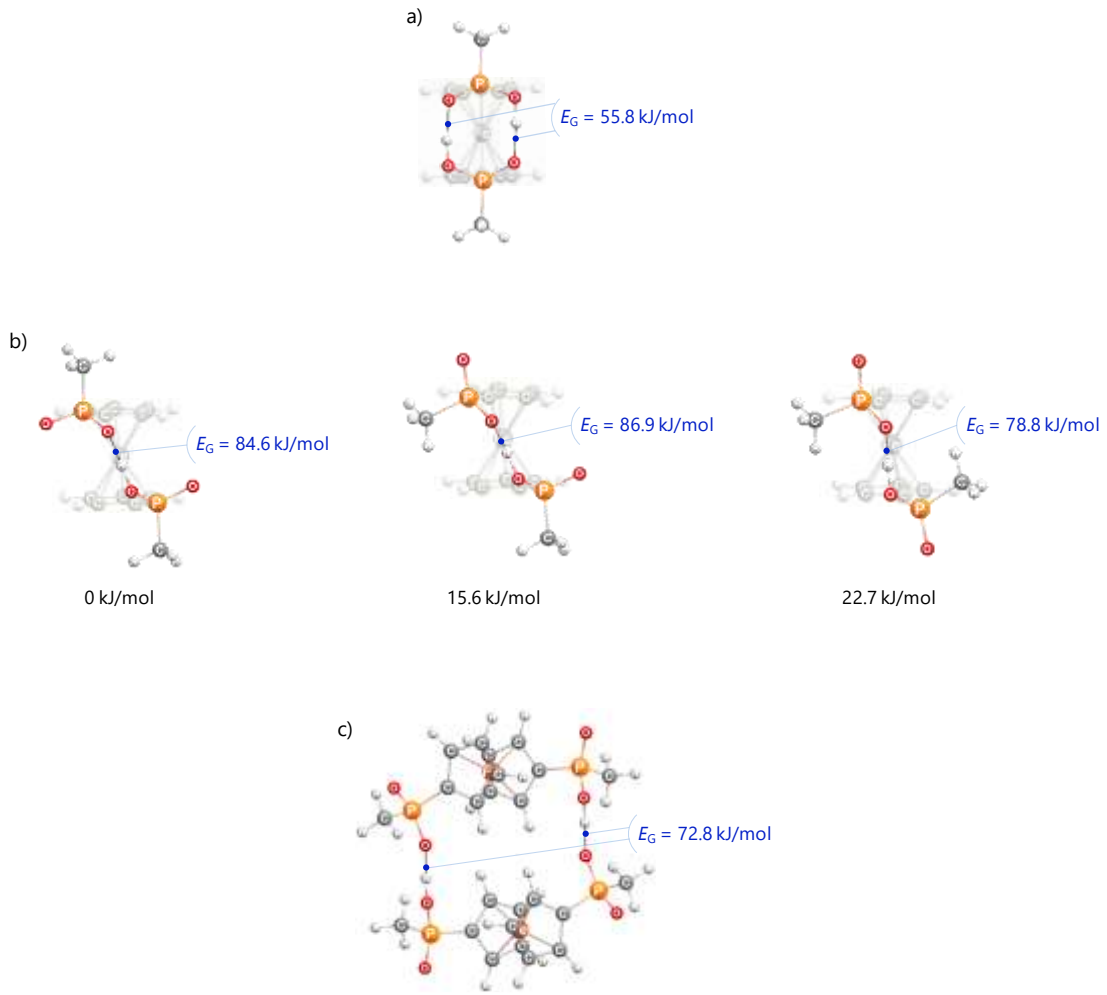

Figure S5. The QTAIM analysis of electron density (in vacuum) at the POH···OP bond critical points (marked in blue) in the FcPMe intramolecular cyclic dimer (a), three isomers of the FcPMe homoconjugated anion (b) with corresponding values of relative total electronic energies (marked in black) and the FcPMe double monoanion (c). The values of local electron kinetic energy density were converted into the values of interaction energy according to the formula given in [Vener et al. *J. Comput. Chem.*, 2012, 33, 2303–2309. DOI: 10.1002/jcc.23062]:

$$E_G = 0.429\ G,$$

where G is in kJ/(mol·Å^3). The same approach was employed in [Espinosa et al. *Chem. Phys. Lett.*, 1998, 285, 170–173. DOI: 10.1016/S0009-2614(98)00036-0], [Mata et al. *Chem. Phys. Lett.*, 2011, 507, 185–189. DOI: 10.1016/j.cplett.2011.03.055], [Kostin et al. *Phys. Chem. Chem. Phys.*, 2022, 24, 7121–7133. DOI: 10.1039/d1cp05939d].

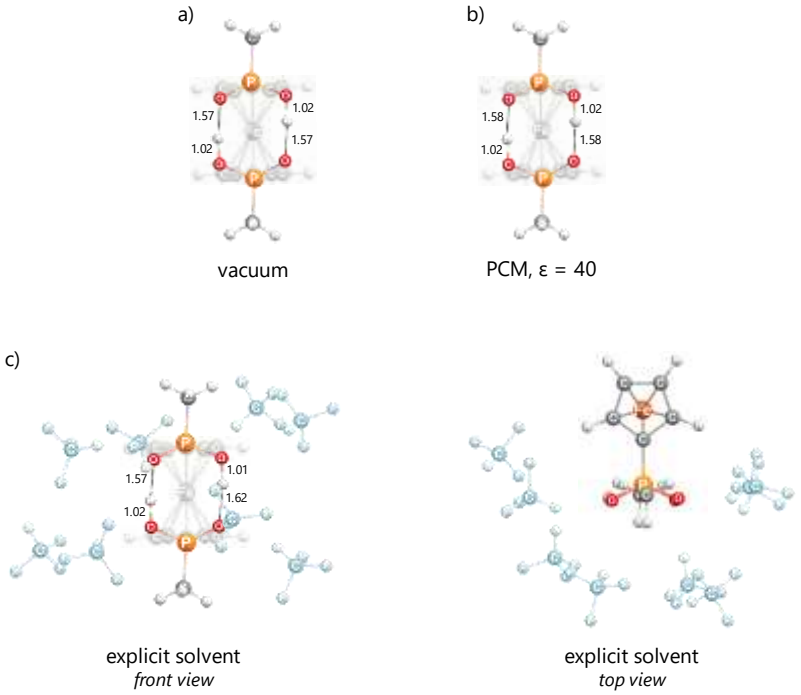

Figure S6. Optimized structures of the FcPMe intramolecular cyclic dimer in vacuum (a), in polarizable continuum (implicit solvation, IEFPCM with ε = 40) (b) and in the medium of eight CHF_3 solvent molecules enveloping the POH···OP bond ring (explicit solvation model) (c). The OH interatomic distances are given in Å. Both implicit and explicit solvation models slightly elongate the OHO bonds.

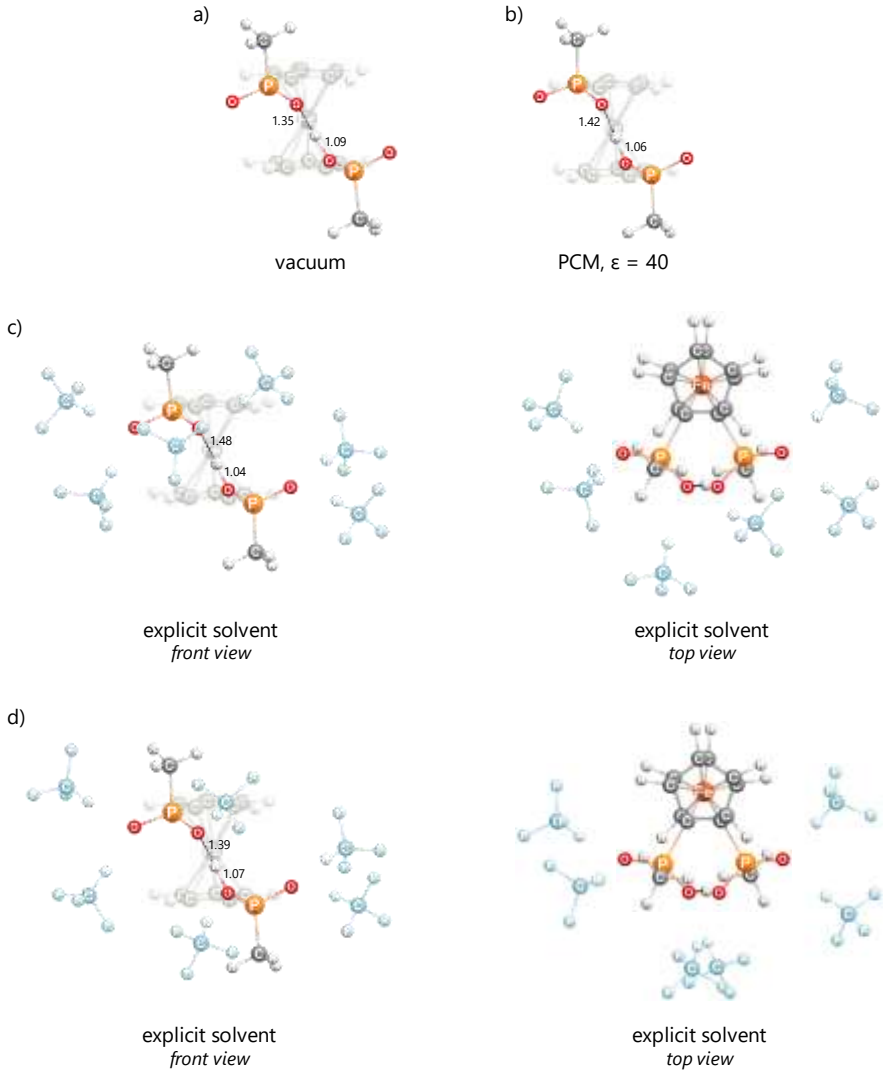

Figure S7. Optimized structures of the FcPMe intramolecular homoconjugated anion in vacuum (a), in polarizable continuum (implicit solvation, IEFPCM with ε = 40) (b) and in the medium of six CHF_3 solvent molecules enveloping the $PO^{-}\cdots HOP$ bond in two possible ways (explicit solvation model) (c and d). The OH interatomic distances are given in Å. Implicit solvent effects lead to a noticeable increase in the $PO^{-}\cdots HOP$ bond length compared to vacuum mainly due to the preferential stabilization of the structure with a more localized negative charge. However, in the case of explicit solvation the $PO^{-}\cdots HOP$ bond length strongly depends on the solvent shell configuration.

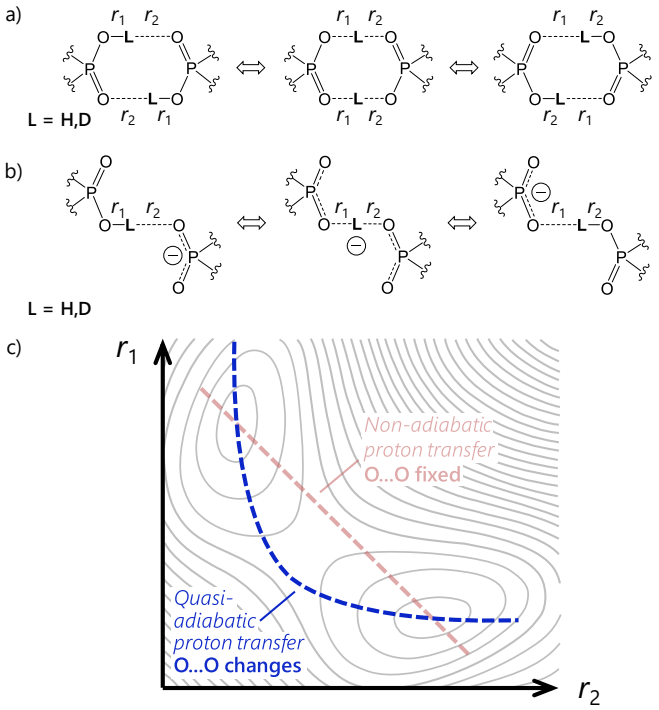

Figure S8. Schematic representations of the bridging particle (proton or deuteron) transfer pathways for the FcPMe intramolecular cyclic dimer (a) and homoconjugated anion (b) with the continuous change of the overall O…O distance. (c) Schematic representation of the double well potential energy surface with the corresponding ("quasi-adiabatic") bridging particle transfer pathway, shown in blue. The alternative "non-adiabatic" pathway is shown in light red. The surface does not correspond to any calculation and serves as a guide for the discussion.

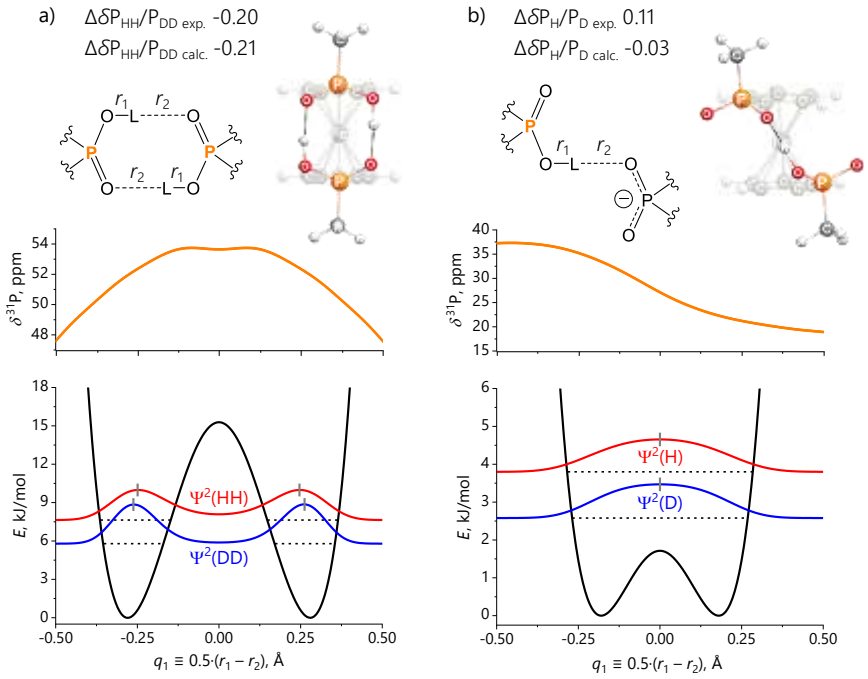

Figure S9. (top) Dependences of the ^{31}P NMR chemical shifts on the proton transfer coordinates q_1, (bottom) double well potentials for the quasi-adiabatic transfer of the bridging particles (protons or deuterons) with the corresponding zero-point vibrational levels and wavefunction squares Ψ^2 for the FcPMe intramolecular cyclic dimer (a) and homoconjugated anion (b). Short grey vertical bars indicate the positions of Ψ^2 maxima.

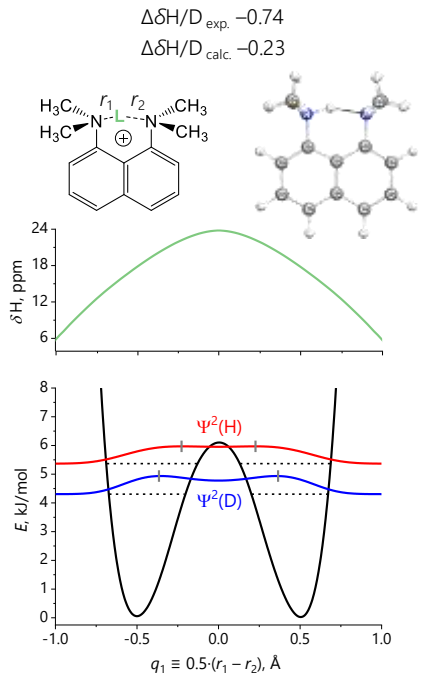

Figure S10. (top) Dependence of the ^{1}H NMR chemical shift on the proton transfer coordinate q_1, (bottom) double well potential for the quasi-adiabatic transfer of the bridging particles (protons or deuterons) with the corresponding zero-point vibrational levels and wavefunction squares Ψ^2 for the DMANH$^+$. Short grey vertical bars indicate the positions of Ψ^2 maxima.

Table S1. Experimental and calculated (equilibrium (eq.) and vibrationally-averaged (av.) according to the quasi-adiabatic pathway) ^{1}H and ^{31}P(*) NMR chemical shifts (in ppm) of the $DMANH^{+}$(**) and the **FcPMe** dimer, homoconjugated anion and double monoanion.

	Experimental		Calculated			
	^{1}H	^{31}P	^{1}H eq.	^{1}H av.	^{31}P eq.	^{31}P av.
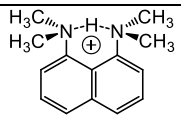	20.64	—	17.81	20.53	—	—
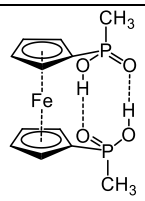	13.47	53.21	12.13	13.98	51.94	52.56
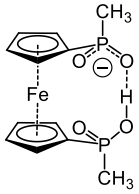	17.36	32.15	16.11	17.20	27.88	27.64
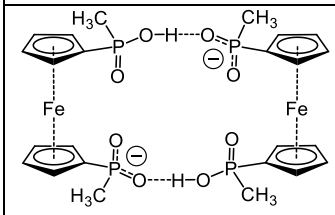	16.96	—	15.17	—	15.92	—

* Note, that the calculated values of ^{31}P NMR chemical shifts ought not to be directly compared with the experimental ones because of the inherent difference in the chemical shift standard referencing: isolated H_3PO_4 molecule in calculations and 85% H_3PO_4 in H_2O solution in experiment.

** The computational procedure was the same as for the **FcPMe** (please refer to section **Quantum-chemical calculations: bridging particle transfer pathways** in the main text); see the potential energy profile, vibrational levels and wavefunctions for H and D, as well as ^{1}H chemical shift function in Figure S10.